

# Performance of Single Spin-Echo and Doubly-Refocused Diffusion-Weighted Sequences in the Presence of Eddy Current Fields with Multiple Components Compared Using Affine Registration

R. G. Nunes<sup>1</sup>, I. Drobniak<sup>2</sup>, S. Clare<sup>3</sup>, P. Jezzard<sup>3</sup>, and M. Jenkinson<sup>3</sup>

<sup>1</sup>Robert Steiner MRI Unit, Imaging Sciences Department, MRC Clinical Sciences Centre, Hammersmith Hospital, Imperial College London, London, United Kingdom, <sup>2</sup>Centre for Medical Image Computing, University College London, London, United Kingdom, <sup>3</sup>Oxford Centre for Functional Magnetic Resonance Imaging of the Brain, University of Oxford, Oxford, United Kingdom

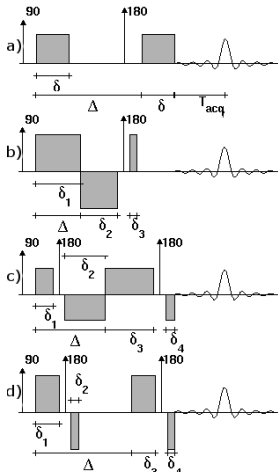


Fig. 1: Simulated sequences: a) standard SE; b) modified SE; c) DSE; d) modified DSE.

**Introduction:** To study fiber structure in the brain using Diffusion-Weighted (DW) Imaging, a set of images corresponding to different diffusion directions are collected. Unfortunately, eddy current fields induced by the strong diffusion gradients can persist throughout the readout window, resulting in significant geometric distortions in echo planar images (EPI) [1], leading to errors in the estimated diffusion parameters. To minimize eddy current fields, several modifications to the standard spin-echo (SE) sequence (Fig.1a) have been proposed. The doubly-refocused sequence (DSE) can null eddy currents with a specific time constant [2] – Fig.1c. Recently, a new implementation has been suggested for when two dominant eddy currents with very different time constants are present, with the timings of the two gradient pairs adjusted independently [3] – Fig.1d. To avoid a second refocusing pulse, a modification to the SE sequence has also been proposed [4] – Fig.1b. The aim of this work is to compare the performance of these four pulse sequences regarding the level of eddy currents produced for the more typical case of several components with dissimilar time constants being present, and to quantify the effectiveness of affine registration in correcting for the resulting image distortions. A realistic MR simulator was used as it enables full control of the amplitudes and time constants of the eddy current components. **Methods:** The MRI simulator POSSUM was used [5]. The algorithm is based on the Bloch equations and models the behavior of the magnetization vector for each small volume element of the brain and tissue type independently, using a 3D digital brain phantom [6]. It is assumed that no significant relaxation effects occur during RF excitation, modeled as a simple rotation of the magnetization vector. The effect of the 180° pulses is simulated by inverting the polarity of the eddy current fields as appropriate: prior to the 180° pulse for SE sequences; in-between pulses for the DSEs. A limitation of this approach is that the interaction between eddy current fields along the slice select direction and the refocusing pulses is not accounted for. The EPI parameters were: field-of-view (FOV) 240x240 mm<sup>2</sup>, in-plane resolution 2x2 mm<sup>2</sup>, 20 slices (4 mm thickness, 2 mm gap), bandwidth 214 kHz, readout window 105 ms, TE 86 ms, 62.5% partial k-space. Homodyne image reconstruction was performed [7]. The gradient timings for the SE sequence were:  $\delta/\Delta$  14/45 ms, amplitude  $G_{diff}$  42 mT/m (b-value 1030 s/mm<sup>2</sup>). These values were based on a standard DW-SE sequence implemented on a Philips Achieva. Eddy currents were simulated by superimposing a sum of exponentially decaying terms to the sequence gradients:  $\sum(\pm)G_{diff}(\pm)\epsilon \exp[-(t-t_i)/\tau]$ . Each term corresponds to switching either on (+) or off (-) the positive or negative diffusion gradients at time  $t_i$ . Time constants of 1, 10 and 100 ms were considered, chosen to represent the different time scales seen on typical scanners. Eddy currents along the readout (x), phase encode (y) and slice directions (z) and B0 eddy currents were simulated. Firstly, to verify that the modified sequences behaved as expected, the gradient timings were optimized so as to null eddy currents with each simulated time constant in isolation, and the gradient amplitudes adjusted to produce the same b-value. Simulations were performed in the presence of three components with the different time constants. All possible combinations for relative amplitudes  $\epsilon$  0.01% and 0.1% were considered with the highest amplitude component targeted in the optimization. When multiple components had the same weight, the one with the longest time constant was nulled. Following optimization, the eddy current fields were inverted as described above. A FLAIR image was also simulated [10]. To reflect the use of an inversion pulse to null CSF, the signal generated for each type of tissue for the non-DW case was multiplied by the factor  $1-2\exp(-TI/T1)$ , with TI 1781 ms, and using POSSUM's default T<sub>1</sub> values at 1.5T [5]: 2569 ms (CSF), 500 ms (WM) and 833 ms (GM). The distorted DW images were registered (affine transformation) to both undistorted T<sub>2</sub>-weighted and FLAIR images with FLIRT [9] using the correlation ratio cost function. To provide the DW images with a different contrast and signal intensity, the mean attenuation in each tissue was considered. Anisotropic diffusion was not modelled. The k-space data corresponding to CSF, white (WM) and gray matter (GM) were separately generated and appropriate attenuation factors applied before summation. These were based on a simple exponential decay and mean diffusivities:  $3.2 \times 10^{-3}$  mm<sup>2</sup>/s (CSF),  $0.8 \times 10^{-3}$  mm<sup>2</sup>/s (GM),  $0.7 \times 10^{-3}$  mm<sup>2</sup>/s (WM) [8]. To evaluate the ability to correct for eddy-current-induced distortions, the sum of the absolute residuals between each registered image and an undistorted DW image was calculated. To provide a standard against which to compare these residuals, two images were generated by applying a small rotation (1° around z, axis in the center of the FOV) or translation (one voxel displacement along x) to the undistorted DW image.

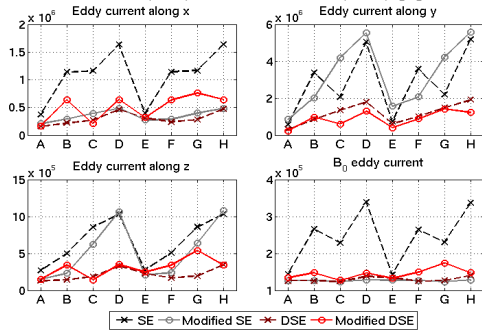


Fig. 2- Sum of absolute residuals following registration to the FLAIR image. Eight amplitude combinations: A (0.01,0.01,0.01), B (0.01,0.01,0.1), C (0.01,0.1,0.01), D (0.01,0.1,0.1), E (0.1,0.01,0.01), F (0.1,0.01,0.1), G (0.1,0.1,0.01), H (0.1,0.1,0.1). Each entry corresponds to the amplitude of the 1, 10 or 100 ms components. Amplitude units are expressed in percentage of the diffusion gradient amplitude (x, y, z eddies) or should be multiplied by 1.5 nT (B0).

registered image and an undistorted DW image was calculated. To provide a standard against which to compare these residuals, two images were generated by applying a small rotation (1° around z, axis in the center of the FOV) or translation (one voxel displacement along x) to the undistorted DW image. **Results and Discussion:** For all modified sequences (Fig. 1b-d), it was possible to adjust the gradient timings so as to null eddy currents with a single component. In the presence of multiple components, the expected distortions were produced: a skew in the xy plane (eddy current along x); image scaling along y (y eddy), skew in the yz plane (z eddy) and a translation along y (B0) [1]. Plots of the residuals obtained after registration to the FLAIR image are shown in Fig. 2. For comparison, the residuals obtained after applying small transformations to the undistorted DW image were:  $7.8 \times 10^5$  (rotation) and  $2.1 \times 10^6$  (translation). Registration to the T<sub>2</sub>-weighted image led to higher residuals compared to prior to registration, which for eddy currents along x, z and B0 were in the order of  $2.0 \times 10^6$  for all tested combinations and all but the SE sequence (not shown). Looking at the images, this was caused by an incorrect scaling caused by the different contrast of the surrounding CSF (bright on the T<sub>2</sub>-weighted, dark on the DWIs). This effect was avoided by using the FLAIR image as target [11]. In this case, residuals were reduced for the standard SE sequence after registration (from a maximum of  $2.7 \times 10^6$  to  $1.6 \times 10^6$ ). The residuals measured for the standard SE were always the highest except for y eddy currents, when the modified SE sequence performed worst in a few cases. On closer inspection, this was related to using a partial acquisition. Although reduced distortions were seen when using this sequence compared to the standard SE, larger gradients were required to achieve the same b-value, leading to larger k<sub>y</sub> shifts. Depending on the polarity of the diffusion gradients (first gradient negative or positive), more or less of the k-space center was sampled resulting in higher image intensities and lower resolution, as in Fig. 2, or signal loss. The two DSE sequences performed better than the single SE sequences, except for combinations B, D, F-H in which case the modified SE sequence performed marginally better than the modified DSE sequence. Comparing the two DSE sequences, similar or slightly lower residuals were measured for Reese's implementation, apart from cases C, D and H for y eddies. When low distortions were visible in the images (modified SE and DSE sequences) registration led to higher residuals. This may be related to interpolation errors. Nevertheless, as the residuals were mostly of the same order as those measured following a small translation, this suggests that image alignment should always be performed as motion-related changes can easily lead to larger errors. **Conclusions:** By using DSE sequences, the distortion effects for equally strong eddy currents are in general substantially reduced when compared with single SE approaches. When the use of an extra refocusing pulse is not advisable, the modified SE sequence [4] should be considered in preference to the standard SE sequence. Image registration should always be performed as motion can easily result in significantly higher errors. **Acknowledgements:** MRC for funding. **References:** [1] Jezzard P et al., MRM,1998;39:80; [2] Reese T et al., MRM,2003;49:177; [3] Finsterbusch J, ISMRM,2009;1380; [4] Finsterbusch J, MRM,2009;61:748; [5] Drobniak I et al, MRM,2006;56:364; [6] Collins DL et al, IEEE Trans Med Imaging,1998;17:463; [7] Noll DC et al, IEEE Trans Med Imaging,1991;10:154; [8] Le Bihan D et al., JMRL,2001;13:534; [9] Jenkinson M et al., NeuroImage,2002;17:825; [10] Hajnal J et al., J Comput Assist Tomogr,1992;16:841; [11] de Crespigny AJ, ISMRM,1998;661.